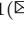# Robust Detection of Circles in the Vessel Contours and Application to Local Probability Density Estimation

Luis Alvarez[1(✉)], Esther González[1], Julio Esclarín[1], Luis Gomez[2],
Miguel Alemán-Flores[1], Agustín Trujillo[1], Carmelo Cuenca[1], Luis Mazorra[1],
Pablo G. Tahoces[3], and José M. Carreira[4]

[1] CTIM, Departamento de Informática y Sistemas, Universidad de Las Palmas de Gran Canaria, Las Palmas, Spain
{lalvarez,esther.gonzalez,julio.esclarin,miguel.aleman,
agustin.trujillo,carmelo.cuenca,lmazorra,luis.gomez}@ulpgc.es
[2] CTIM, Dpto. de Ingeniería Electrónica y Automática, Universidad de Las Palmas de Gran Canaria, Las Palmas, Spain
[3] CITIUS, Universidad de Santiago de Compostela, A Coruña, Spain
{pablo.tahoces,josemartin.carreira}@usc.es
[4] Complejo Hospitalario Universitario de Santiago (CHUS), A Coruña, Spain

Abstract. In this work we propose a technique to automatically estimate circular cross-sections of the vessels in CT scans. First, a circular contour is extracted for each slice of the CT by using the Hough transform. Afterward, the locations of the circles are optimized by means of a parametric snake model, and those circles which best fit the contours of the vessels are selected by applying a robust quality criterion. Finally, this collection of circles is used to estimate the local probability density functions of the image intensity inside and outside the vessels. We present a large variety of experiments on CT scans which show the reliability of the proposed method.

Keywords: Vessels · Circle Hough transform · Seed point · Histogram analysis · CT images

1 Introduction

Most of the techniques for the segmentation of vessels require seed points inside the vessels and an analysis of the intensity histogram to separate the vessels from the surrounding tissues. For instance, in [1], the authors use an initial circle inside the aortic lumen and two intensity thresholds for CT images in order to track the geometry of the aortic lumen by using an elliptical model of its cross-sections. In [4], the authors propose a region growing-based strategy for vessel segmentation which starts by manually placing one or more seed points in the vessel(s) of interest. From these seed points, more neighboring voxels are included in the segmentation using some image intensity thresholds. In [7], a

review of 3D techniques for the segmentation of the vessel lumen is presented. In particular, some of the techniques which are studied use probability distribution models of the aorta and the surrounding tissues.

The usual way to automatically compute a seed point inside the vessels consists in using the Hough transform to search for circular vessel contours. In [2], the authors propose the Hough transform to automatically locate a circle in the descending aorta in MR images. In [8], the authors propose to use the most caudal image slice to locate the position of the aorta using the Hough transform. In [9], the authors propose to use the Hough transform to detect the ascending aorta using the prior knowledge about the expected range for the diameter of the ascending aorta (from 22 mm to 34 mm).

In this paper we propose to combine the Hough transform with the following parametric snake model proposed in [6] to estimate accurately circle locations:

$$E(R, \bar{c}) = \frac{1}{2\pi} \int_0^{2\pi} \nabla I_\sigma(C(\theta)) \cdot \bar{n}(\theta) d\theta \tag{1}$$

$$+ \alpha_- \left(\frac{\iint_{A_-} (I_\sigma(C(\theta)) - I_-)^2 r dr d\theta}{|A_-|} \right)^{\frac{1}{2}} + \alpha_+ \left(\frac{\iint_{A_+} (I_\sigma(C(\theta)) - I_+)^2 r dr d\theta}{|A_+|} \right)^{\frac{1}{2}}$$

where $C(\theta) = (c_x + R \cdot cos(\theta), c_y + R \cdot sin(\theta))$, I_σ is the original image convolved with a Gaussian kernel, $\alpha_-, \alpha_+ \geq 0$, A_-, A_+ are annulus in both sides of the circle contour, and I_-, I_+ are the average of I_σ in A_-, A_+. The local minima of this energy correspond to circles which fit high image contrast areas. We point out that, using the Hough transform, the locations of the circle centers and their radii are usually given in integer (or low) precision. Using the circles provided by the Hough transform as initialization, the application of the parametric snake model improves the accuracy of the circle locations and provides a measure of the quality of the circles. The lower the value of $E(R, \bar{c})$, the higher the quality of the circle. In fact, in this paper we combine several circle quality estimators to select the "best" circle along the image slices in a robust way. By measuring the similarity with the "best" circle, we select a collection of circles which correspond to vessel contours. This collection of circles is used to estimate, in a local way, the probability density functions of the intensity inside and outside the vessels by using a kernel density estimation. We point out that these probability distributions are very useful pieces of information for the automatic segmentation of the vessels.

The main contributions of this paper are:

- A new method for the automatic and robust computation of a collection of circular cross-sections of the vessels based on the combination of the Hough transform, a snake parametric model and a new quality criterion for the circle selection. The centers of such circles can be used as seed points for the automatic segmentation of vessels.
- A new technique for the kernel density estimation of the local probability density functions inside and outside the vessels based on the sampling of the image intensity values inside the collection of circles and in a neighborhood

of those circles. We point out that, as the collection of circles is distributed along the slices of the 3D image, by considering a neighborhood around each circle, we obtain a reliable sample of the intensities in a neighborhood of the whole vessel.

The rest of the paper is organized as follows: In Sect. 2, we present the proposed method to compute a collection of circles on the vessel contours. In Sect. 3, we study how to estimate the probability density distributions of the image intensity values inside and outside the vessels. In Sect. 4, we present some experiments and, in Sect. 5, we present the main conclusions.

2   Detection of Circles in the Vessel Contours

Let I be a $3D$ image consisting of N slices. That is, $I = \{I^z\}_{z=1,..,N}$. For each slice I^z, using the circle Hough transform, we compute the most voted circle, C^z, with center (c_x^z, c_y^z) and radius R^z for a range of circle radii in the interval $[R_{min}, R_{max}]$ (in the experiments presented in this paper we use $R_{min} = 5\,\text{mm}$, $R_{max} = 15\,\text{mm}$). The locations of such circles are then optimized to fit the vessel contour by minimizing the energy criterion proposed in [6] (equation (6)) using a parametric snake model. From the collection of circles $\{C^z\}$, we select, in a robust way, the "best" one by combining several quality criteria. The main goal is that the contour of the selected circle belongs to the vessel contour with a high probability. The quality criteria we use are:

1. The voting score V^z, provided by the Hough transform. The higher the value of V^z, the better.
2. The circle energy E^z, provided by the method proposed in [6], which measures how well the circle fits an image contour. The lower the value of E^z, the better.
3. The standard deviation σ^z of the image intensity values I^z inside the circle. We assume that the variation of the image intensity inside the vessel is low, so that the lower the value of σ^z, the better.
4. In general, the location of the circles C^z across the sequence is expected to be stable in the slices of the CT scan where the vessel contours have a circular shape. Therefore, we use the distance D^z between the circle centers (c_x^z, c_y^z) and (c_x^{z+1}, c_y^{z+1}) as quality measure. Since this estimation is very local, we convolve $\{D^z\}$ with a Gaussian kernel to obtain a more reliable estimation. The lower the value of D^z, the better.

Next, we combine the above quality measures in the following way to obtain a robust and reliable circle quality criterion Q^z:

$$Q^z = \frac{V^z}{median\{V^z\}} - \frac{E^z}{median\{E^z\}} - \frac{\sigma^z}{median\{\sigma^z\}} - \frac{D^z}{median\{D^z\}}. \quad (2)$$

The higher the value of Q^z, the better the circle. Then we select the "best" reference circle $C^{z_{opt}}$ as the one which maximizes Q^z. We observe that we can include different weights as parameters in the combination of the quality criteria

in the definition of Q^z. However, to simplify the exposition, in this paper we use the fixed combination given by the above equation.

Once the reference circle $C^{z_{opt}}$ has been obtained, we use it to select, by similarity, a collection of circles $\{C^{z_i}\} \subset \{C^z\}$ which belong to the vessel contours. We assume that C^{z_i} lies entirely inside the vessel if Q^{z_i} is big enough and the mean and standard deviation of the image intensity values inside C^{z_i}, μ^{z_i} and σ^{z_i} respectively, are similar to those for $C^{z_{opt}}$. That is,

$$\{C^{z_i}\} = \{C^z : Q_z > p_Q \text{ and } \frac{|\mu^z - \mu^{z_{opt}}|}{\mu^{z_{opt}}} < p_\mu \text{ and } \frac{|\sigma^z - \sigma^{z_{opt}}|}{median\{\sigma_z\}} < p_\sigma\}, \quad (3)$$

where $p_Q, p_\mu, p_\sigma > 0$ are parameters of the algorithm. We point out that, with the proposed approach, we avoid the detection of circles on non-vascular structures, as shown in the experimental results. Indeed, there exist other organs, like the trachea or the backbone, where the CT cross-sections may have a circular shape. However, with our approach, the circles in the trachea are not selected because they correspond to dark circles surrounded by a brighter background (and the proposed method looks for the opposite, that is, bright circles in a darker background). In the backbone, the standard deviation of the image intensity inside the circle is much higher than in the vessels, so that our quality criterion penalizes such circles with respect to the circles in the vessels.

3 Application to the Local Analysis of the Histogram Around the Vessels

Let $\{C^{z_i}\}$ be the collection of circles in the vessel contours estimated using the proposed method. Given $\lambda > 0$, we define $C_\lambda^{z_i}$ as the circle with the same center as C^{z_i} and area equal to $\lambda \cdot AREA(C^{z_i})$. Based on the collection of circles $\{C_\lambda^{z_i}\}$, we define the sample S_λ, of the image intensity values as

$$S_\lambda = \{I^{z_i}(x) : x \in C_\lambda^{z_i}\}. \quad (4)$$

We use a kernel density estimation (KDE) to approximate the probability density function of the sample S_λ. That is, the kernel density estimator is

$$\hat{f}_h^\lambda(s) = \frac{1}{|S_\lambda|h} \sum_{s_k \in S_\lambda} K\left(\frac{s - s_k}{h}\right), \quad (5)$$

where $K(\cdot)$ is the kernel (in this paper we use the normal distribution $N(0,1)$ as $K(\cdot)$) and h is the bandwidth (in the experiments we fix the value of h to 5). We point out that $\hat{f}_h^1(s)$ is an approximation of the probability density inside the vessels and $\hat{f}_h^2(s)$ is an approximation of the probability density in a local neighborhood of the vessels. Next, from $\hat{f}_h^1(s)$ and $\hat{f}_h^2(s)$, we estimate the probability density of the image intensity values in S_2 outside the vessels, $\hat{g}_h^{1,2}(s)$. First we observe that

$$\hat{f}_h^2(s) = a\hat{f}_h^1(s) + (1 - a)\hat{g}_h^{1,2}(s), \quad (6)$$

where $a > 0$, is the proportion of points in S_2 which are inside the vessels. To estimate a, we assume that, locally, there are no points outside the vessels with an intensity value close to the median of the intensity values inside the vessels. That is, we assume that $\hat{g}_h^{1,2}(s) \approx 0$ for $s \in [p_1, p_2]$, where p_1, p_2 are percentile values of $\hat{f}_h^1(s)$ around its median (in the experiments shown in this paper, we use p_1 as the 40th percentile value and p_2 as the 60th percentile value). Then, we estimate a as

$$a = median \left\{ \frac{\hat{f}_h^2(s)}{\hat{f}_h^1(s)} \right\}_{s \in [p_1, p_2]}. \tag{7}$$

Once a is estimated, we approximate $\hat{g}_h^{1,2}(s)$ as

$$\hat{g}_h^{1,2}(s) = \frac{1}{M} \max \left\{ \frac{\hat{f}_h^2(s) - a\hat{f}_h^1(s)}{1 - a}, 0 \right\}, \tag{8}$$

where $M > 0$ is fitted in such a way that $\hat{g}_h^{1,2}(s)$ integrates to one.

4 Experimental Results

First, we study the ability of criterion (2) to obtain robust and reliable circles in the contours of the vessels. To obtain the initial circle in each slice, we use a gradient-based Hough transform which takes into account that, in a CT scan, the intensity values are usually brighter inside the vessels than in the surrounding tissues. For comparison purposes, we also use a standard implementation of the Hough transform. In our dataset, we use 10 high-quality contrast-enhanced MDCT scans provided by the University Hospital Complex of Santiago de Compostela (CHUS) and 332 contrast-enhanced scans from the database LIDC-IDRI (see [3,5]). This database has been designed for lung cancer screening and the images are, in general, of poor quality for our purpose.

In Table 1, we show the region where the reference circle is located when we use the standard Hough circle transform maximizing the voting score, and when we apply the proposed method maximizing the circle quality score Q^z.

Table 1. Location of the reference circle obtained by maximizing the voting score using the standard Hough circle transform, and by using the proposed method maximizing the circle quality score Q^z for the image databases we use.

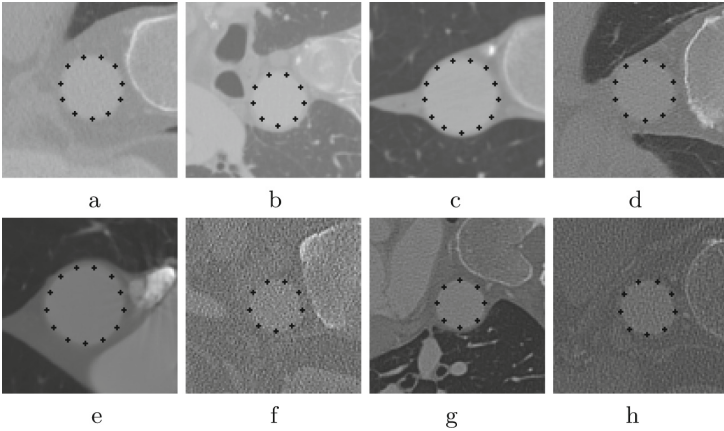|	aorta	innominate trunk	backbone	trachea	other
Standard Hough (CHUS database)	9	0	1	0	0
Proposed method (CHUS database)	10	0	0	0	0
Standard Hough (LIDC database)	238	1	44	32	17
Proposed method (LIDC database)	324	8	0	0	0

Fig. 1. Circle obtained by maximizing Q^z along the image slices for 8 images of the LIDC-IDRI database.
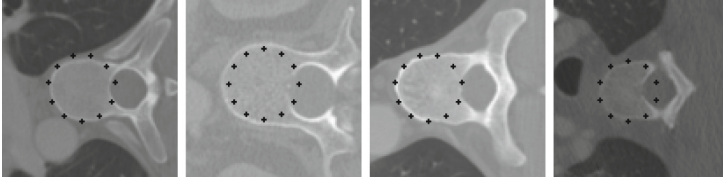

Fig. 2. Examples of images of the LIDC-IDRI database where the circle which maximizes the standard Hough transform is located in the backbone.

We point out that, in the backbone and in the trachea, the image contours may have a circular shape and the standard Hough transform could therefore provide the reference circle in these areas. In a CT scan, the image intensity inside the trachea is darker than outside it, so that the proposed method never selects the trachea contour as circle because we assume that the intensity is brighter inside the circle than outside it in the gradient-based Hough implementation. On the other hand, in the quality criterion Q^z, we consider the standard deviation of the image intensity and the stability of the position of the circle across the sequence. In general, these estimators are lower inside the vessel than in the backbone, which reduces the probability of attaining the minimum of Q^z in the backbone. In Fig. 1, we show the circle obtained by maximizing Q^z along the image slices for 8 CT scans of LIDC-IDRI database. In Fig. 2, we show 4 images of the LIDC-IDRI database where the circle which maximizes the standard Hough transform is located in the backbone. In Fig. 3, we show 4 images of the LIDC-IDRI database where the circle which maximizes the standard Hough transform is located in the trachea. Another limitation of the standard Hough transform is that, in some cases, the circle which maximizes the voting score cannot properly fit the vessel contours. This is illustrated in Fig. 4. This lack of accuracy is solved
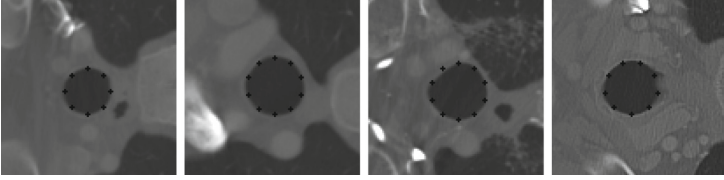
Fig. 3. Examples of images of the LIDC-IDRI database where the circle which maximizes the standard Hough transform is located in the trachea.
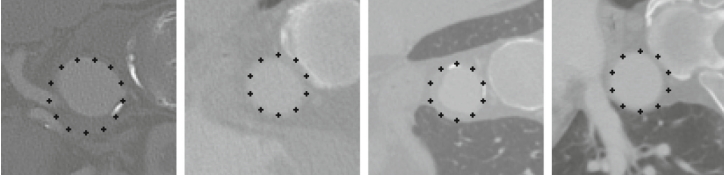

Fig. 4. Examples of images of the LIDC-IDRI database where the circle which maximizes the standard Hough transform does not properly fit the vessel contours.

in the proposed method in 2 ways. On the one hand, we consider the standard deviation of the image intensity inside the circle and, on the other hand, we improve the circle location using the parametric snake model introduced in [6]. In Fig. 5, for one tomography of CHUS database, we show 8 out of 234 circles selected by similarity with the reference one using criterion (3). All 234 circles are inside the vessels, most of them in the aorta. The first selected circle is in the innominate trunk and the last one is in the iliac artery. We point out that we consider that our method works properly if all selected circles are inside the vessels.
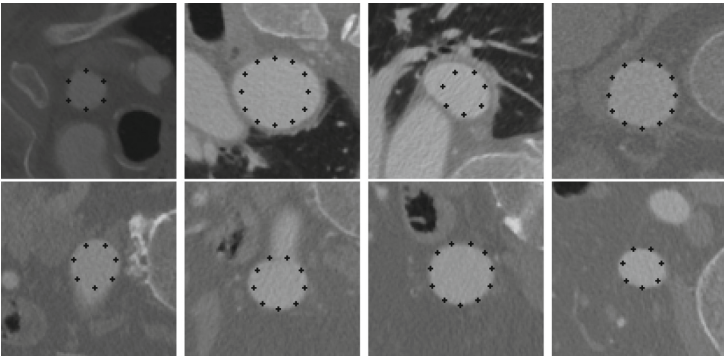

Fig. 5. Examples of some of the 234 circles selected by similarity with the reference one using criterion (3) for one image of the CHUS database.

In Fig. 6, we show, for 4 images of the CHUS database, the KDE of the probability distribution of the image intensity inside the vessels $(\hat{f}_h^1(s))$, in a neighborhood of the vessels $(\hat{f}_h^2(s))$, and outside the vessels $(\hat{g}_h^{1,2})$, computed using the proposed approach. We observe that the value of a is close to 0.5. This is due to the fact that the size of the sample S_2 in the vessel neighborhood is the double of the area of the sample S_1 inside the vessels.
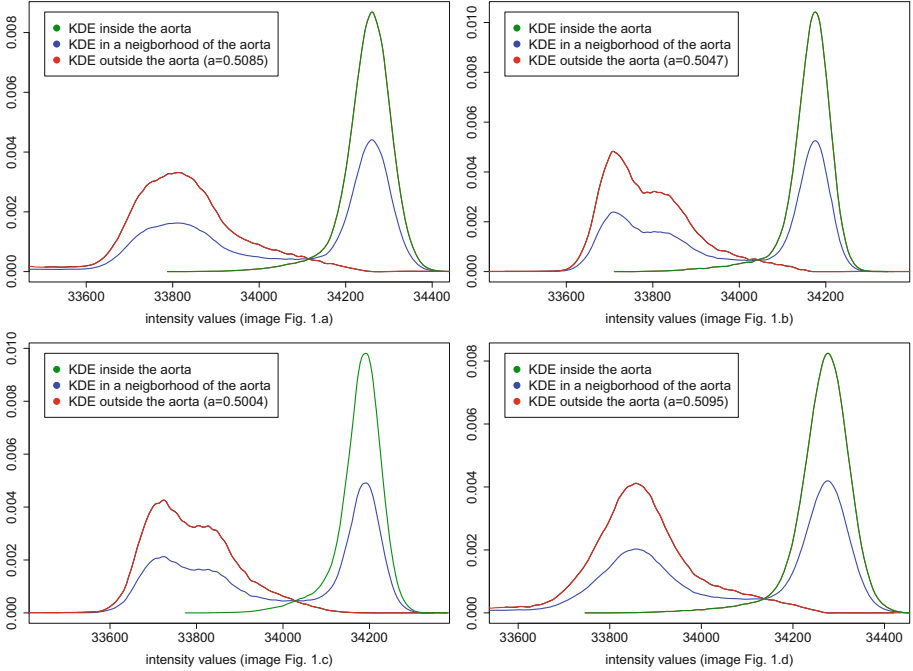

Fig. 6. KDE of the probability distribution of the image intensity inside the vessels, $\hat{f}_h^1(s)$, in a neighborhood of the vessels, $\hat{f}_h^2(s)$, and outside the vessels, $\hat{g}_h^{1,2}(s)$, computed using the proposed approach for 4 images of the CHUS database. For each case, we also show the estimated proportion of vessel points, a, using (7).

5   Conclusions

In this paper we propose a new method for the automatic and robust compu-
tation of a collection of circles in the vessel contours and a quality criterion for
the circle selection. From this information, we compute the KDE of the local
probability density function inside and outside the vessels, which can be very
useful in vessel segmentation techniques. Moreover, the centers of the selected
circles can be used as seed points inside the vessels. As shown in the experi-
mental results, the Hough transform voting score alone is not a reliable criterion
for circle selection. The circle quality criterion proposed in this paper provides

a much more robust estimation and the results in a large variety of CT scans are very promising. The shapes of the KDE estimations, shown in Fig. 6, suggest that the usual normal distribution model to approximate the probability distribution inside the vessels is not very accurate. This is likely due to the fact that the image intensity values are lowered near the boundary of the vessels because of the influence of the surrounding tissues.

References

1. Alvarez, L., Trujillo, A., Cuenca, C., González, E., Esclarín, J., Gomez, L., Mazorra, L., Alemán-Flores, M.G., Tahoces, P., Carreira, J.M.: Tracking the aortic lumen geometry by optimizing the 3D orientation of its cross-sections. In: MICCAI 2017 (2017, to appear)
2. Adame, I.M., van der Geest, R.J., Bluemke, D.A., Lima, J.A., Reiber, J.H., Lelieveldt, B.P.: Automatic vessel wall contour detection and quantification of wall thickness in in-vivo MR images of the human aorta. J. Magn. Reson. Imaging **24**(3), 595–602 (2006)
3. Armato, S.G., et al.: The lung image database consortium (LIDC) and image database resource initiative (IDRI): a completed reference database of lung nodules on CT scans. Med. Phys. **38**(2), 915–931 (2011)
4. Boskamp, T., Rinck, D., Link, F., Kmmerlen, B., Stamm, G., Mildenberger, P.: New vessel analysis tool for morphometric quantification and visualization of vessels in CT and MR imaging data sets. RadioGraphics **24**(1), 287–297 (2004)
5. Clark, K., Vendt, B., Smith, K., Freymann, J., Kirby, J., Koppel, P., Moore, S., Phillips, S., Maffitt, D., Pringle, M., Tarbox, L., Prior, F.: The cancer imaging archive (TCIA): maintaining and operating a public information repository. J. Digit. Imaging **26**(6), 1045–1057 (2013)
6. Cuenca, C., González, E., Trujillo, A., Esclarín, J., Mazorra, L., Alvarez, L., Martínez-Mera, J.A., Tahoces, P.G., Carreira, J.M.: Fast and accurate circle tracking using active contour models. J. Real-Time Image Process. 1–10 (2015)
7. Lesage, D., Angelini, E.D., Bloch, I., Funka-Lea, G.: A review of 3D vessel lumen segmentation techniques: models, features and extraction schemes. Med. Image Anal. **13**(6), 819–845 (2009)
8. Martínez-Mera, J.A., Tahoces, P.G., Carreira, J.M., Suárez-Cuenca, J.J., Souto, M.: A hybrid method based on level set and 3D region growing for segmentation of the thoracic aorta. Comput. Aided Surg. **18**(5–6), 109–117 (2013)
9. Wang, S., Fu, L., Yue, Y., Kang, Y., Liu, J.: Fast and automatic segmentation of ascending aorta in MSCT volume data. In: 2009 2nd International Congress on Image and Signal Processing, pp. 1–5, October 2009